Sonocrystallization Hot Paper

DOI: 10.1002/ange.201408894

# Sonocrystallization Yields Monoclinic Paracetamol with Significantly Improved Compaction Behavior**

*Dejan-Krešimir Bučar,* James A. Elliott,* Mark D. Eddleston, Jeremy K. Cockcroft, and William Jones*

***Abstract:*** *Ultrasound-assisted crystallization (sonocrystallization) was used to prepare a mixture of nano- and micrometer-sized crystals of the monoclinic form of paracetamol—a widely used analgesic known for its particularly problematic mechanical behavior under compression (i.e. poor tabletability). The nano- and micrometer-sized crystals yielded a powder which exhibits elastic moduli and bulk cohesions that are significantly higher than those observed in samples consisting of macrometer-sized crystals, thus leading to enhanced tabletability without the use of excipients, particle coating, salt, or cocrystal formation. Experimental compaction and finite element analysis were utilized to rationalize the significantly improved compaction behavior of the monoclinic form of paracetamol.*

The current demand for organic nanomaterials[1,2] has triggered the development of fabrication methods for organic nanocrystals.[3–10] Recent pharmaceutical and biomedical research has shown that molecular nanocrystals are highly valuable in the context of drug delivery, biolabeling, and biosensing.[11,12] Nanosizing of molecular crystals has also become a particularly popular approach in drug development with poorly soluble pharmaceutical agents[13] and is mainly used to enhance the solubility and bioavailability of the drug candidate.[14,15] Surprisingly, other applications of molecular crystals, despite their unique physicochemical properties, have been relatively unexplored in biomedical (and other) sciences. We show herein through the use of sonocrystallization,[16,17] that is, the use of ultrasound to facilitate crystallization,[18] that nanometer-sized crystals can significantly improve the mechanical properties of a crystalline pharmaceutical agent.

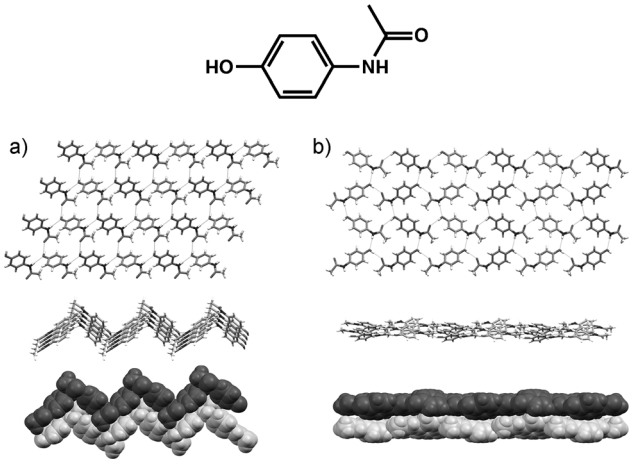


***Figure 1.*** Chemical structure of **pca** (top) and the crystal structures of a) form I (monoclinic, stable) and b) form II (orthorhombic, metastable) featuring corrugated and flat molecular sheets found in their respective crystal structures. The crystal packing diagrams (bottom) of forms I and II are viewed along the crystallographic axes *c* and *a*, respectively.

Paracetamol (**pca**, Figure 1), also known as acetaminophen, is an exceptionally popular analgesic and antipyretic that achieves annual sales of more than one billion US dollars in the United States alone.[19] Two polymorphs of **pca** are well known—the monoclinic[20] form I and the orthorhombic[21] form II. An elusive and metastable polymorph, form III, has only recently been structurally characterized.[22] The thermodynamically stable form I exhibits poor tabletability under compression.[23,24] The orthorhombic form II, on the other hand, displays significantly better compaction properties,[23,25] but is thermodynamically less stable[26,27] and, thus, not ideal for drug formulation and commercialization. The poor tabletability of form I is attributed to its crystal structure. In particular, form I is based on corrugated hydrogen-bonded layers of **pca** molecules and lacks the presence of flat molecular layers that can promote the formation of microscopic slip planes capable of rendering the crystalline solid plastic and easier to compact (Figure 1a).[23] Form II, on the other hand, exhibits slip planes comprised of flat hydrogen-bonded **pca** layers[21] that promote better tabletability (Figure 1b).

Marketed **pca** tablets are generally formulated using the poorly compactible monoclinic form I along with up to

[*] Dr. D.-K. Bučar, Dr. J. K. Cockcroft
Department of Chemistry, University College London
20 Gordon Street, London WC1H 0AJ (UK)
E-mail: d.bucar@ucl.ac.uk
Dr. J. A. Elliott
Department of Materials Science and Metallurgy
University of Cambridge
27 Charles Babbage Road, Cambridge CB3 0FS (UK)
E-mail: jae1001@cam.ac.uk
Dr. M. D. Eddleston, Prof. W. Jones
Department of Chemistry, University of Cambridge
Lensfield Road, Cambridge CB2 1EW (UK)

[**] D.K.B. acknowledges the Royal Society for a Newton International Fellowship and University College London for an UCL Excellence Fellowship. D.K.B. and W.J. thank the Isaac Newton Trust (Trinity College, University of Cambridge) for funding. J.A.E. would like to thank M. Bennett, M. House, and W. Bertram of Huxley Bertram for the use of their compaction simulator. W.J. and M.D.E. acknowledge support by the Interreg IV "2 Mers Seas Zeeën" cross-border cooperation program 2007–2013.

Supporting information for this article is available on the WWW under http://dx.doi.org/10.1002/anie.201408894.

  

25 wt% of excipients to reduce the occurrence of defective tablets, such as through capping, lamination, or chipping.[28] The poorly compactible crystals of form I can also be coated with hydroxypropylcellulose to improve their behavior under compression.[29] Alternatively, **pca** can be formulated as a salt[30] or cocrystal[31] to facilitate the assembly of crystal structures that contain slip planes that result in improved tabletability.

A recent study has shown that freeze-drying water/acetone solutions of **pca** leads to the formation of microcrystals of form I with enhanced compaction properties.[32] Specifically, it was demonstrated that tablets based on submicrometer-sized crystals exhibit a high compressive strength of 40 MPa (axially) and about 6 MPa (diametrally), as well as a low porosity of 6%. Such tablets, however, need to be prepared using a compaction pressure of 345 MPa—which exceeds those typically used in industrial tableting processes (in the range 100–170 MPa) to limit damage to dies and tooling.[33] Furthermore, it was suggested that the freeze-drying method is not economically viable for inexpensive drugs such as **pca.**[32]

We show herein that time- and cost-efficient ultrasound-assisted crystallization yields sub-micrometer- and micrometer-sized crystals of form I which exhibit elastic moduli and bulk cohesions that are significantly higher than those observed in macrocrystalline form I, thereby giving rise to a remarkable increase in tabletability at compaction pressures that are typically used in current industrial processes. We also reveal that mechanochemically prepared nanocrystals (using liquid-assisted grinding as a production method) exhibit narrower particle-size distributions and are not as tabletable as the sonocrystallized solid, thus suggesting that particle-size distribution may play a significant role in the improvement of the compaction behavior of form I.

Combined sonication and fast precipitation afforded the formation of a physical mixture of nano- and microcrystals of form I. In a typical sonocrystallization experiment, **pca** was dissolved in a minimal amount of ethanol to obtain a solution, which was immediately injected through a syringe filter into hexane while being exposed to ultrasound. The suspension was sonicated for 1 min, filtered, and dried at room temperature. The obtained solid was analyzed by powder X-ray diffraction (PXRD), selected-area electron diffraction (SAED), scanning-electron microscopy (SEM), and transmission electron microscopy (TEM). Details of the synthesis and analysis are provided in the Supporting Information.

A PXRD analysis of the sonocrystallized bulk material, in addition to SAED measurements of individual nanocrystals, revealed that **pca** crystallizes as form I (Figure 2a–c). The presence of the orthorhombic form II could not be detected by PXRD and SAED. A thorough inspection of the SEM and TEM images indicated that the sonocrystallized sample exhibits a broad particle-size distribution. Specifically, the micrographs revealed the presence of aggregated nano- and micrometer-sized crystals with plate and prism morphologies and prismatic crystals in the bulk (Figure 2d–h, and see Figures S3–S6 in the Supporting Information). The micrographs also showed that the crystals are uniform in shape, with particle sizes ranging from about 0.14 μm to 40 μm in length. The thickness of the crystal plates was estimated on the basis of TEM images to be as low as about 200 nm. A particle-size distribution analysis was attempted using dynamic light scattering (DLS) and powder X-ray diffraction (PXRD). The DLS results indicated that the nano- and microcrystals form aggregates with an average diameter of 60 μm. Although crystal agglomeration can be prevented by the use of surfactants, we have not considered the use of surfactants to characterize the sonocrystallized solid, as they

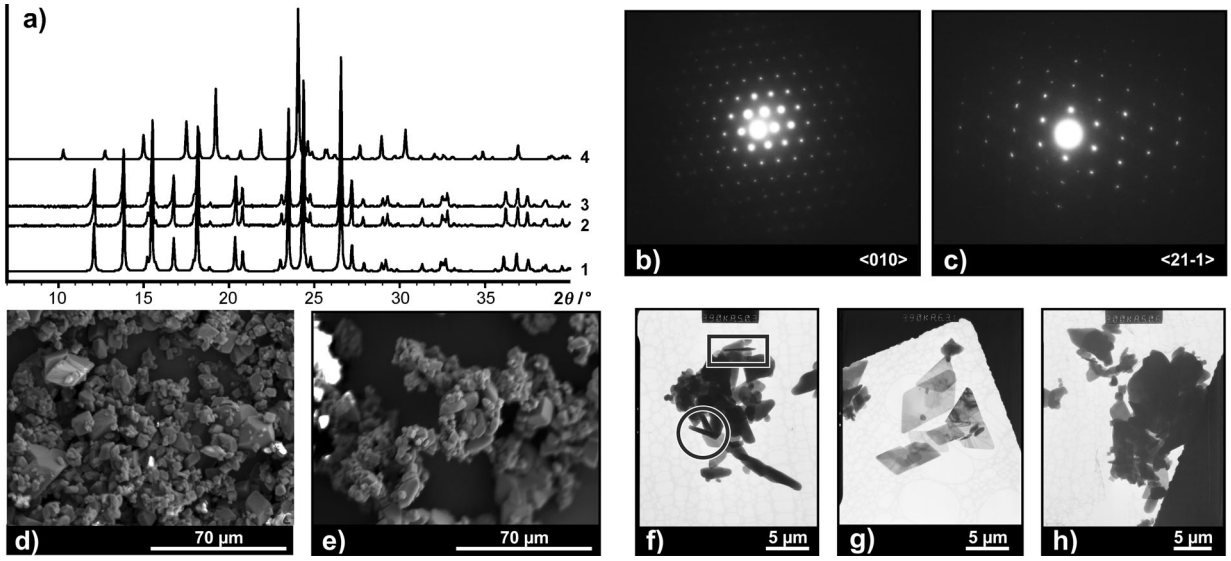


***Figure 2.*** Crystallographic characterization of the sonocrystallized bulk of form I: a) PXRD patterns of **pca** (1: calculated form I, 2: sonocrystallized form I, 3: sonocrystallized form I after compaction, 4: calculated form II) and b,c) SAED patterns obtained from individual nanodimensional single crystals, which are consistent with the formation of form I (b: ⟨010⟩ zone axis, c: ⟨21-1⟩ zone axis). The SEM and TEM images shown in (d–h) depict sonocrystallized nano- and microparticles of form I which exhibit broad particle-size distributions. Nanocrystalline plates with a measured thickness of 220–230 nm (rectangle) and 470–590 nm (circle) are highlighted in (f).

are known to alter the crystal size and morphology.[34] The PXRD data did not reveal any measurable peak broadening that could be attributed to the presence of nanocrystals in the bulk. This observation is consistent with the broad particle-size distribution of the sample and the presence of micrometer-sized crystals in the sonocrystallized bulk material.

To evaluate the compaction behavior of commercial (i.e. macrocrystalline) and sonochemically (i.e. nano-/microcrystalline) prepared batches of form I, we utilized a hydraulic uniaxial compaction simulator with an instrumented die (Huxley Bertram), which allowed the simultaneous measurement of axial and radial stresses and, ultimately, stress–density curves for the studied materials. Relevant parameters relating to the mechanical properties of the solids are shown in Table 1, wherein they are also compared to those of Avicel PH101 (a pharmaceutical-grade microcrystalline cellulose commonly used as a binder to hold the ingredients in a tablet together).

***Table 1:*** Material parameters for powders characterized by compaction simulator using DPC constitutive model.

| Material | Young's modulus ($E$) [MPa] | Cohesion ($d$) [MPa] |
|---|---|---|
| Avicel (PH101) | 3700 | 4.2 |
| **pca** (commercial) | 2612 | 0.1 |
| **pca** (sonocrystallized) | 6365 | 3.4 |

As expected, it was observed that tablets formed from the commercial **pca** sample crumbled on ejection from the die.[23,24,35] In contrast, the tablets made from sonocrystallized **pca** retained their sharp edges (Figure 3a, inset). A comparison of the stress–density curves for sonocrystallized and commercial **pca** is shown in Figure 3a. It can be seen that, during the unloading phase, the sonocrystallized form I obtained a higher relative density than the macrocrystalline form at the same applied pressure, thus indicating that more plastic deformation had taken place. The final relative densities of tablets after ejection from the die were 0.922 (7.8% porosity) and 0.866 (13.4% porosity), respectively. In other words, the tablet formed from the sonocrystallized material is more than 40% less porous than the tablet formed from macrocrystalline powder under the same conditions.

Compaction simulations using the Drucker–Prager cap constitutive model (see the Supporting Information) revealed that particles of sonocrystallized form I exhibit higher elastic moduli than particles of the macrocrystalline sample (Table 1). The higher elastic modulus suggests that sonocrystallized form I should store a greater amount of elastic energy on deformation, thus leading to poor compaction properties. The improved tabletability of sonocrystallized form I is, however, attributed to its greater compactability (i.e. higher relative density under a given load) and the greater amount of plastic energy dissipated during compaction. Both of these effects feasibly arise indirectly from the nanosized particles, with their greater total contact area between particles, which thus increases their cohesion and packing density compared to the macrocrystalline sample. Despite an apparent increase in the elastic modulus of the sonocrystallized form I relative to the macrocrystalline form (by a factor of 2.4, see Table 1), the vastly increased cohesion (by a factor of 34, see Table 1) and extra plasticity during deformation mean that tablet fracture as a result of elastic recovery on decompression is less likely in the tablet made from sonocrystallized powder.

A TEM study on the tableted powder of the sonocrystallized batch of form I was also carried out to determine whether a polymorphic phase transition had occurred that could lead to the improved compaction behavior. For this purpose, we cut a tablet in half, and investigated only the solid that crumbled off the halved tablet and had, thus, not been in contact with the utilized tools. A PXRD measurement

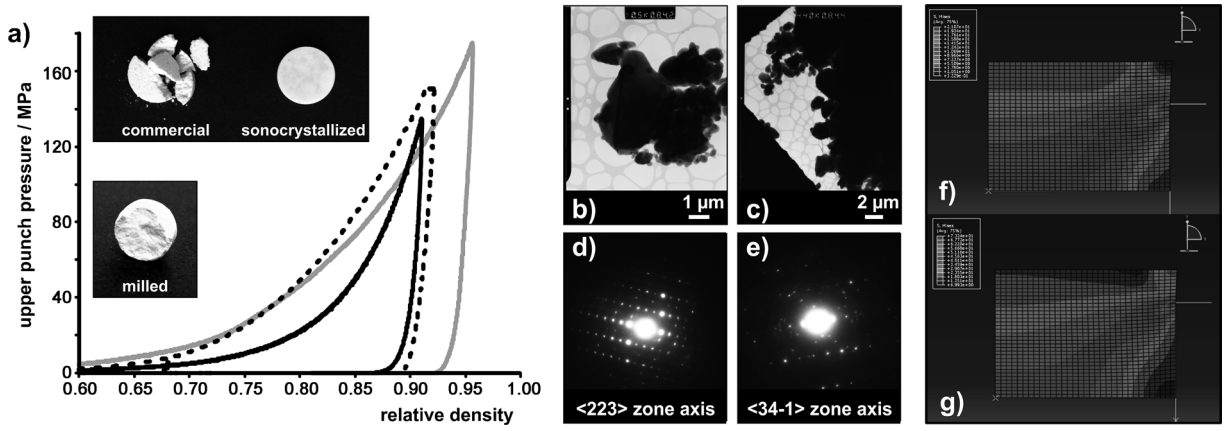


***Figure 3.*** a) Comparison of stress–density curves for macrocrystalline (black), sonocrystallized (gray), and milled (dotted black) form I. The relative density refers to the powder density relative to the density of the crystal structure of form I ($\rho = 1.263\ g\,cm^{-3}$; inset: tablets composed of commercial, sonocrystallized, and milled form I after compaction); b,c) TEM images showing that the compacted nano- and microcrystals of form I shattered into smaller particles; d,e) SAED patterns obtained from individual nanodimensional compacted single crystals, which reveal that compaction has led to an increase in crystal defects, but no phase transition; f,g) stress distributions calculated from axisymmetric finite element simulations of cylindrical tablets comprised of macrocrystalline form I (f) and nanocrystalline form I (g) during ejection from the die (the top of the die wall is indicated by a horizontal white line on the far right-hand side of the figures, and the left-hand side is the axis of the die, about which the simulation is cylindrically symmetrical).

  

showed that the solid still consisted exclusively of form I crystals (Figure 2a). In addition, TEM images and corresponding SAED patterns (Figure 3b–e) showed that the investigated crystals correspond to form I. The observed crystals are considerably smaller in size (ca. 1 μm along all the crystal axes) (Figure 3b,c), thus indicating that the nano- and microcrystals cracked into smaller particles during the compaction process. This is further evidenced by SAED experiments that revealed that the crystals exhibited a significantly higher degree of mosaicity (Figure 3d,e) compared to those prior to compaction. Moreover, a PXRD trace of the compacted material revealed broadening of the diffraction peaks, which is consistent with a decrease of the particle size of the material (average particle size: ca. 1.5 μm, see the Supporting Information).

To assess the behavior of **pca** under high pressure, axisymmetric finite element simulations of cylindrical tablets during ejection from the die were used to calculate the stress distributions (Mises deviatoric stress, in MPa) within the compacted commercial and sonocrystallized solid. Figure 3f,g shows the stress distributions for commercial (i.e. macrocrystalline) and sonocrystallized (i.e. nano-/micrometer-sized) **pca** at the same point during simulation, and shows that the stress distribution is more inhomogeneous for the commercial solid, especially near the edges of the tablet. Based on previous findings from tableting simulations using pharmaceutical excipients,[36] this would suggest that tablets made from macrocrystalline **pca** would be more likely to chip or fail mechanically during the ejection phase.

The above-described results raised the question of whether the mechanical properties of form I can be further improved by preparing even smaller crystals that are also uniform in size. To evaluate this possibility, we turned to liquid-assisted grinding[37,38]—a mechanochemical method used to generate high-shear and impact forces for making uniform nanodimensional crystals.[39] In a typical experiment, a macrocrystalline batch of form I was milled in the presence of hexane. PXRD was used to identify the milled **pca** sample as form I, while PXRD and SEM were used to define the sample as nanocrystalline and more uniform (compared to sonocrystallized **pca**), with an average particle size of 1 μm (details of the PXRD particle-size analyses are provided in the Supporting Information).

The compaction studies showed that tablets made from milled **pca** crumbled on ejection from the die, as seen in the case of commercial **pca** (see Figure 3a, inset). Similarly to the sonocrystallized solid, the milled material consisted exclusively of form I crystals that had decreased in size upon exposure to the high pressures (average particle size: 0.9 μm, see the Supporting Information). Furthermore, the stress–density curve of the milled sample exhibited a relative density of 0.891 (10.9% porosity), which is higher than that of the commercial sample (0.866, 13.4% porosity), but lower than that of sonocrystallized **pca** (0.922, 7.8% porosity). It is interesting to compare the behavior of the sonocrystallized and milled samples, both of which contain appreciable amounts of nanosized crystals (Figures 2 and 3; see also the Supporting Information). Despite this similarity, Figure 3 shows that the load curve for milled form I (dotted line) differs significantly from both macrocrystalline and sonocrystallized samples (black and gray, respectively). In particular, the sonocrystallized sample reaches a higher maximum relative density (i.e. lower porosity) for loads exceeding 40 MPa, and has a larger hysteresis on unloading, thus indicating that a greater amount of mechanical work is lost to plastic deformation or fracture of particles on compaction. The increased propensity for the plastic deformation of nanometer-sized crystals is known for metallic systems,[40] and may also be a contributing factor to the improved tabletability of the sonocrystallized and milled form I over the commercial macrocrystalline solid. The origin of the poorer compaction properties of the milled solid compared to those of the sonocrystallized solid remains, at this point, to be fully understood.

To conclude, we have shown that **pca** form I, an analgesic and antipyretic known for its poor tabletability, can be crystallized using a combination of ultrasonication and fast precipitation to obtain a mixture of nano- and macrocrystals that display significantly improved tabletability at pressures that are typically used in current industrial processes, and in the absence of any excipients. The superior tabletability is attributed to the enhanced ability of the solid to plastically deform and the significantly higher cohesive interactions between its particles than those observed in the macrocrystalline samples. We have also shown that milled form I (consisting of smaller uniform particles) displays compaction properties that are inferior to those observed for the sonocrystallized material, thus suggesting the possibility that a broader particle-size distribution promotes the tabletability of **pca.** We believe that the presented results demonstrate the utility of sonocrystallization in the preparation of pharmaceutically relevant molecular nano-/microcrystals with superior properties. Studies are underway to evaluate the impact of particle size and distribution on the mechanical properties of other organic solids obtained using bottom-up (e.g. sonocrystallization) and top-down (e.g. milling) methods.

Received: September 8, 2014
Published online: November 4, 2014

**Keywords:** crystal growth · nanostructures · polymorphism · powder compaction · sonocrystallization

[1] *Single Organic Nanoparticles* (Eds.: H. Masuhara, H. Nakanishi, K. Sasaki), Springer, Berlin, **2003**.
[2] *Organic Nanomaterials: Synthesis Characterization, and Device Applications* (Eds.: T. Torres, G. Bottari), Wiley-VCH, Weinheim, **2013**.
[3] V. Monnier, N. Sanz, E. Botzung-Appert, M. Bacia, A. Ibanez, *J. Mater. Sci.* **2006**, *16*, 1401 – 1409.
[4] E. Kwon, H. Oikawa, H. Kasai, H. Nakanishi, *Cryst. Growth Des.* **2007**, *7*, 600 – 602.
[5] J. R. G. Sander, D.-K. Bučar, J. Baltrusaitis, L. R. MacGillivray, *J. Am. Chem. Soc.* **2012**, *134*, 6900 – 6903.
[6] B. Sinha, R. H. Müller, J. P. Möschwitzer, *Int. J. Pharm.* **2013**, *453*, 126 – 141.
[7] D.-K. Bučar, L. R. MacGillivray, *J. Am. Chem. Soc.* **2006**, *129*, 32 – 33.

  

[8] J. R. G. Sander, D.-K. Bučar, R. F. Henry, G. G. Z. Zhang, L. R. MacGillivray, *Angew. Chem. Int. Ed.* **2010**, *49*, 7284 – 7288; *Angew. Chem.* **2010**, *122*, 7442 – 7446.
[9] C. Karunatilaka, D.-K. Bučar, L. R. Ditzler, T. Friščić, D. C. Swenson, L. R. MacGillivray, A. V. Tivanski, *Angew. Chem. Int. Ed.* **2011**, *50*, 8642 – 8646; *Angew. Chem.* **2011**, *123*, 8801 – 8805.
[10] D. Yan, D.-K. Bučar, A. Delori, B. Patel, G. O. Lloyd, W. Jones, X. Duan, *Chem. Eur. J.* **2013**, *19*, 8213 – 8219.
[11] H. Kasai, T. Murakami, Y. Ikuta, Y. Koseki, K. Baba, H. Oikawa, H. Nakanishi, M. Okada, M. Shoji, M. Ueda, H. Imahori, M. Hashida, *Angew. Chem. Int. Ed.* **2012**, *51*, 10315 – 10318; *Angew. Chem.* **2012**, *124*, 10461 – 10464.
[12] S. Fery-Forgues, *Nanoscale* **2013**, *5*, 8428 – 8442.
[13] J. P. Möschwitzer, *Int. J. Pharm.* **2013**, *453*, 142 – 156.
[14] E. M. Merisko-Liversidge, G. G. Liversidge, *Toxicol. Pathol.* **2008**, *36*, 43 – 48.
[15] M. Wang, G. C. Rutledge, A. S. Myerson, B. L. Trout, *J. Pharm. Sci.* **2012**, *101*, 1178 – 1188.
[16] M. D. Luque de Castro, F. Priego-Capote, *Ultrason. Sonochem.* **2007**, *14*, 717 – 724.
[17] J. R. G. Sander, B. W. Zeiger, K. S. Suslick, *Ultrason. Sonochem.* **2014**, *21*, 1908 – 1915.
[18] K. S. Suslick, *Science* **1990**, *247*, 1439 – 1445.
[19] W. M. Lee, *Hepatology* **2004**, *40*, 6 – 9.
[20] M. Haisa, S. Kashino, R. Kawai, H. Maeda, *Acta Crystallogr. Sect. B* **1976**, *32*, 1283 – 1285.
[21] M. Haisa, S. Kashino, H. Maeda, *Acta Crystallogr. Sect. B* **1974**, *30*, 2510 – 2512.
[22] M.-A. Perrin, M. A. Neumann, H. Elmaleh, L. Zaske, *Chem. Commun.* **2009**, 3181 – 3183.
[23] G. Nichols, C. S. Frampton, *J. Pharm. Sci.* **1998**, *87*, 684 – 693.
[24] M. Duberg, C. Nyström, *Powder Technol.* **1986**, *46*, 67 – 75.
[25] E. Joiris, P. Martino, C. Berneron, A.-M. Guyot-Hermann, J.-C. Guyot, *Pharm. Res.* **1998**, *15*, 1122 – 1130.
[26] K. Kachrimanis, K. Fucke, M. Noisternig, B. Siebenhaar, U. Griesser, *Pharm. Res.* **2008**, *25*, 1440 – 1449.
[27] T. Beyer, G. M. Day, S. L. Price, *J. Am. Chem. Soc.* **2001**, *123*, 5086 – 5094.
[28] J. S. M. Garr, M. H. Rubinstein, *Int. J. Pharm.* **1991**, *72*, 117 – 122.
[29] C. C. Sun, L. Shi, *Pharm. Res.* **2011**, *28*, 3248 – 3255.
[30] S. R. Perumalla, L. Shi, C. C. Sun, *CrystEngComm* **2012**, *14*, 2389 – 2390.
[31] S. Karki, T. Friščić, L. Fábián, P. R. Laity, G. M. Day, W. Jones, *Adv. Mater.* **2009**, *21*, 3905 – 3909.
[32] A. Ogienko, E. Boldyreva, A. Yu Manakov, V. Boldyrev, A. Yunoshev, A. Ogienko, S. Myz, A. Ancharov, A. Achkasov, T. Drebushchak, *Pharm. Res.* **2011**, *28*, 3116 – 3127.
[33] G. Ragnarsson in *Pharmaceutical Powder Compaction Technology* (Eds.: G. Alderborn, C. Nyström), Marcel Dekkers, New York, **1996**, pp. 77 – 97.
[34] J. P. Canselier, *J. Dispersion Sci. Technol.* **1993**, *14*, 625 – 644.
[35] I. Krycer, D. G. Pope, J. A. Hersey, *J. Pharm. Pharmacol.* **1982**, *34*, 802 – 804.
[36] L. H. Han, J. A. Elliott, A. C. Bentham, A. Mills, G. E. Amidon, B. C. Hancock, *Int. J. Solids Struct.* **2008**, *45*, 3088 – 3106.
[37] D.-K. Bučar, S. Filip, M. Arhangelskis, G. O. Lloyd, W. Jones, *CrystEngComm* **2013**, *15*, 6289 – 6291.
[38] T. Friščić, W. Jones, *Cryst. Growth Des.* **2009**, *9*, 1621 – 1637.
[39] G. D. Wang, F. P. Mallet, F. Ricard, J. Y. Y. Heng, *Curr. Opin. Chem. Eng.* **2012**, *1*, 102 – 107.
[40] H. Zheng, A. Cao, C. R. Weinberger, J. Y. Huang, K. Du, J. Wang, Y. Ma, Y. Xia, S. X. Mao, *Nat. Commun.* **2010**, *1*, 1449.

  